ISSN 0020-1685, Inorganic Materials, 2023. © Pleiades Publishing, Ltd., 2023.
Russian Text © The Author(s), 2023, published in Neorganicheskie Materialy, 2023, Vol. 59, No. 1, pp. 3–9.

Structural and Electronic Properties of $SmGaGe_2O_7$ Studied by First Principles Methods

A. V. Baglov[a, b, *] and L. S. Khoroshko[a]

[b a] *Belarussian State University, Minsk, 220030 Belarus*

[b] *Belarussian State University of Informatics and Radio Engineering, Minsk, 220013 Belarus*

**e-mail: baglov@bsu.by*

Received May 10, 2022; revised July 22, 2022; accepted July 27, 2022

Abstract—The crystal structure and electronic properties of the samarium gallium digermanate $SmGaGe_2O_7$ have been studied for the first time using first principles quantum-mechanical methods. The lattice parameters and the position of ions obtained in the generalized gradient approximation agree with experimental data. The material is shown to be an indirect band gap semiconductor with a band gap of 2.45 eV. Its valence band is formed by oxygen *p*-states, with an insignificant contribution of other states of the other atoms. Its conduction band is formed by gallium and germanium *s*- and *p*-states, with a small contribution of oxygen *p*-states and samarium *d*-states, located ≈1 eV from the conduction band bottom. The material contains charge carriers differing in effective mass.

Keywords: quaternary compounds, germanates, oxides, rare-earth elements, lanthanide, samarium, density functional theory, pseudopotential theory

DOI: 10.1134/S002016852301003X

INTRODUCTION

Recent years have seen increasing research interest in ternary and quaternary germanium oxide compounds (polygermanates)—salts of the corresponding germanium-containing acids [1]. Most interest has been aroused by group 13 metal digermanates with the general formula $M_2Ge_2O_7$, derived from $H_2Ge_2O_7$. The interest in the digermanates is due to potential practical applications of these compounds as materials for laser engineering, phosphors, light-emitting diodes, optical converters, nuclear detectors, etc., as well as to the relative ease of preparing them by solidstate reactions from precursors, usually metal sesquioxides (M_2O_3) and germanium dioxide (GeO_2) [1–8]. In $RMGe_2O_7$ quaternary compounds, R is a rareearth (RE) element, often yttrium, and M is fully or partially replaced by Fe to impart to them magnetic properties. The lanthanide iron quaternary digermanates with the general formula $RFeGe_2O_7$ are distinctive in that they have unusual magnetic and structural properties. The compounds containing yttrium-group RE ions, except for gadolinium, are known to have space group $P2_1/m$ [9, 10]. In the case of cerium-group RE ions, including lanthanum and gadolinium, the compounds have space group $P2_1/c$ [11, 12]. This structural anomaly has not yet been consistently explained. In addition, temperature dependences of magnetic susceptibility for $SmFeGe_2O_7$ have an anomaly related to simultaneous antiferromagnetic ordering of the Fe^{3+} and Sm^{3+} ions [11, 12]. Moreover, the $RFeGe_2O_7$ (R = Tb–Tm) compounds were reported to undergo metamagnetic transitions [9].

However, even though this class of compounds is potentially attractive for practical application, there are insufficient, fragmentary data on their physicochemical properties. Indium yttrium digermanate, $YInGe_2O_7$, has been studied experimentally in greatest detail. Its structure and luminescence properties have been well studied for not only pure crystals but also crystals activated with Sm^{3+} [13], Eu^{3+} [4, 14], Dy^{3+} [15], Tm^{3+} [16], Pr^{3+} [17], and even Bi^{3+} ions [18]. In addition, Drokina et al. [19] studied characteristic features of the magnetic order in $SmFeGe_2O_7$. For a number of compounds, heat

capacity and thermodynamic parameters were reported [20–38]. At the same time, information about the electronic structure of the compounds in question, in particular, that about energy band dispersion, electronic density of states, orbital occupancy, etc., is missing in the literature.

The purpose of this work was to study the crystal structure and electronic properties of the samarium gallium digermanate $SmGaGe_2O_7$ using first principles quantum-mechanical modeling methods. This particular digermanate was chosen because it can be used as a model compound for the $RGaGe_2O_7$ (R = RE element) series and because there are experimental data on its structure for assessing applicability of first

1

Table 1. Main structural parameters of $SmGaGe_2O_7$ crystals

Parameter	Calculated	Measured [30]
a, Å	7.1870(2)	7.18610(9)
b, Å	6.7329(1)	6.57935(8)
c, Å	12.9601(6)	12.7932(2)
β, deg	116.2262	117.4216(6)
V, Å^3	562.57	536.90(1)
ρ, g/cm^3	5.63	5.90

principles modeling methods to structural studies of such compounds [30].

METHOD OF INVESTIGATION

Structural and electronic properties were studied using OpenMX software, which combines density functional theory and pseudopotential theory [39–41]. The starting unit cell was constructed using experimental data [30]. The self-consistent field calculation procedure was thought to be complete if the electronic energy between two sequential iterations was under 10^{-6} eV/ion. In the first Brillouin zone, integration was performed over a Γ-centered 4 × 4 × 2 regular grid of *k*-points. For numerical integration, a 57 × 60 × 102 grid was chosen, which corresponded to an average cut-off energy of 2940 eV. Pseudopotentials included germanium 4*s* and 4*p* electrons, gallium 3*d*, 4*s*, and 4*p* electrons, and oxygen 2*s* and 2*p* electrons as valence electrons. For samarium, we used a so-called opencore pseudopotential in which the 5*s*, 5*p*, 5*d*, and 6*s* electrons were used as valence electrons, and the 4*f* electrons were included in the core. In this process, a partial correcting core charge was generated so that the radial part of the atomic orbitals approached the real one. The basis set was constructed in the form of a linear combination of pseudoatomic orbitals with the use of two optimized basis functions for each valence electron, with one additional optimized basis function as a polarization function to more accurately take into account chemical bonding in crystals and adequately reproduce energy band dispersion. For samarium, whose polarization orbital was not included in the basis set, we used two optimized basis functions for valence electrons and two for core electrons. In numerical simulation, we took into account spin polarization in the generalized gradient approximation using the exchange-correlation functional proposed by Perdew et al. [42]. Since no magnetic ordering was reported for the compound under consideration, we thought it to be an antiferromagnet, like $SmFeGe_2O_7$. The electronic density of states was calculated by the tetrahedron method over a Γ-centered 5 × 5 × 3 regular grid of *k*-points. Before calculating electronic properties, we performed structural optimization (relaxation) of the unit cell with a varied volume and ion sites until any component of the tensor of stresses or forces acting on ions was below 0.01 eV/Å.

RESULTS AND DISCUSSION

Figure 1 shows the optimized unit cell of $SmGaGe_2O_7$. It contains four formula units, has monoclinic symmetry, and is a simple centrosymmetric cell with space group $P2_1/c$, which persists in the process of structural relaxation and is observed in experiments [30]. Note that all of the ions in this compound occupy the same Wyckoff position: 4*e*. This leads us to assume the presence of antisite defects, which can play an important role on the crystal-chemical and crystal-physical properties of the $RMGe_2O_7$ compounds, especially if the digermanates contain ions of 3*d* and/or 4*f* elements. A comparative analysis of calculated and experimentally determined characteristics, such as the lattice parameters, monoclinic angle, Wyckoff position coordinates, unit-cell volume, and density of the material, shows that the quantum-mechanical modeling method chosen here adequately reproduces the experimental data. As is typical of the approximation chosen and the exchange-correlation functional, the bond lengths are overestimated, which leads to slightly overestimated *b* and *c* lattice parameters, by 2.3 and 1.3%, respectively, and a slight decrease in monoclinic angle, by 1.2° (1%), compared to the experimental data (Tables 1, 2). It should be noted that, in the case under consideration, the overestimation is larger than that usually observed for the approximation chosen and the exchange-correlation functional. We suggest that this is due to the inclusion of 4*f* electrons in the core, which rules out their full-scale interaction with the valence electron subsystem, thereby increasing the tendency for bond lengths to be overestimated. At the same time, to the best of our knowledge there are no reports on systematic studies of the effect of 4*f* electrons in terms of the concept of pseudopotential open-core on the accuracy in reproducing structural properties of complex lanthanide compounds or binary lanthanide oxides, so we do not rule out possible effects of other factors.

The band structure of the digermanate is shown in Fig. 2. Along high-symmetry points, we observe a large number of bands, which can be divided into two groups differing in the number of bands and separated by an energy gap of 2.45 eV. The energy is measured from the valence band top. At a depth of –2 eV, we observe a large number of bands about 0.2–0.3 eV in width, with low dispersion. The valence band top is located not in the center of the Brillouin zone but on a lateral face at point Y_2. There is another, 40 meV lower band at this point. In addition, there is a local extremum at point *A*, 10 meV below the valence band top (Fig. 2, upper inset). Given that two bands arrive at this point and that there are two, closely spaced bands at point Y_2 as well, we assume the presence of charge carriers with several different effective masses. The conduction band is formed by a smaller number of bands, 0.6 to 1.8 eV in width, with lower dispersion. The conduction band bottom is located in the center of the Brillouin zone, thus the digermanate is

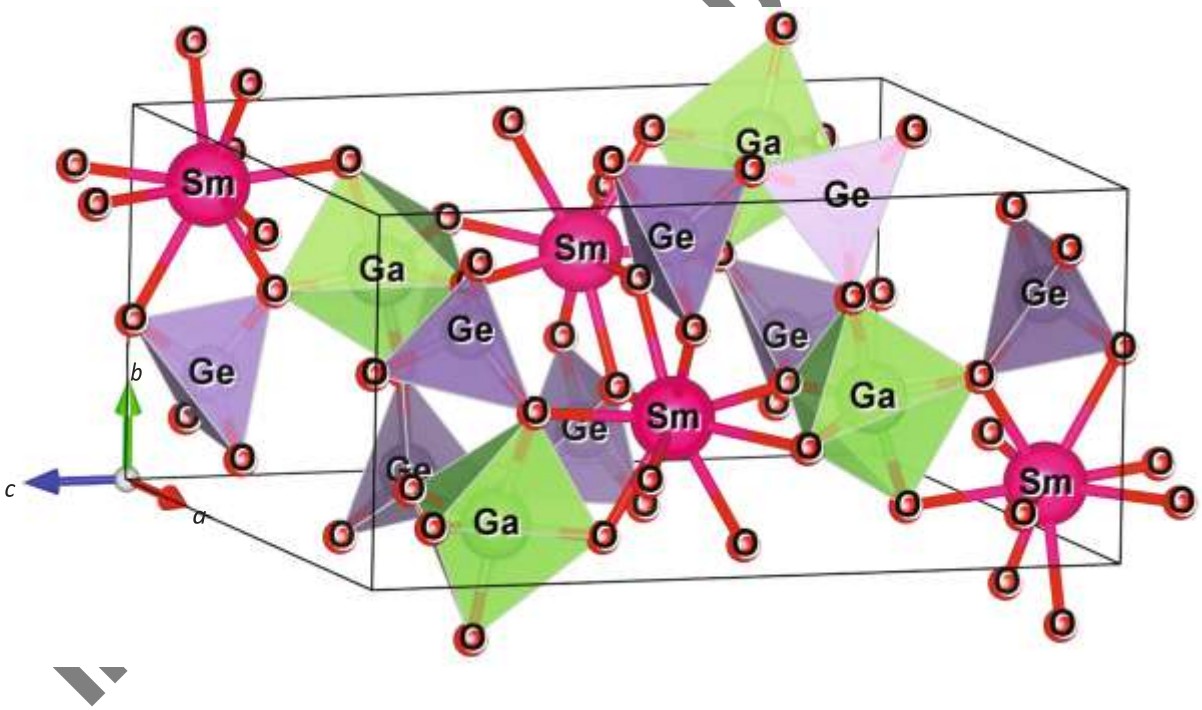

Fig. 1. Unit cell of the samarium gallium digermanate $SmGaGe_2O_7$.

INORGANIC MATERIALS 2023

Table 2. Inequivalent ion position coordinates in $SmGaGe_2O_7$ crystals

Ion	*x*	*y*	*z*
Sm	0.762096 0.7607 2( )	0.145322 0.14692 19( )	0.023300 0.02845 12( )
Ga	0.792508 0.7893 4( )	0.401311 0.3998 5( )	0.267577 0.2689 2( )
Ge(1)	0.785349 0.7837 4( )	0.657484 0.6566 4( )	0.039638 0.0435 2( )
Ge(2)	0.296302 0.2993 4( )	0.412149 0.4100 4( )	0.221646 0.2215 2( )
O(1)	0.587808 0.5896 18( )	0.827947 0.8308 19( )	0.016425 0.0191 9( )
O(2)	0.793688 0.7782 15( )	0.108256 0.115 2( )	0.219716 0.2181 10( )
O(3)	0.568260 0.5674 16( )	0.374225 0.383 2( )	0.308222 0.3064 10( )
O(4)	0.007606 0.0047 18( )	0.339362 0.3285 19( )	0.424354 0.4208 10( )
O(5)	0.748032 0.746 2( )	0.004880 0.0005 16( )	0.420696 0.4226 11( )
O(6)	0.793479 0.7947 18( )	0.446773 0.4488 15( )	0.124369 0.1307 11( )
O(7)	0.148365 0.154 2( )	0.187953 0.1867 17( )	0.182763 0.1870 12( )

Calculated and experimentally determined coordinates over and under the bar, respectively [30].

an indirect band gap material. Owing to the appreciable dispersion, the extrema at the other points lie 1.2 to 1.8 eV higher, except for point *B* (0.55 eV higher). Since the Y_2–Γ and *B*–Γ transitions differ in height by just 10 meV, both transitions are assumed to take part in determining the electrical transport properties of the compound.

Figure 3a shows the atom-projected electronic density of states (DOS) obtained by summing all states for each type of atom, and Fig. 3b shows orbital-projected electronic DOS obtained by summing states

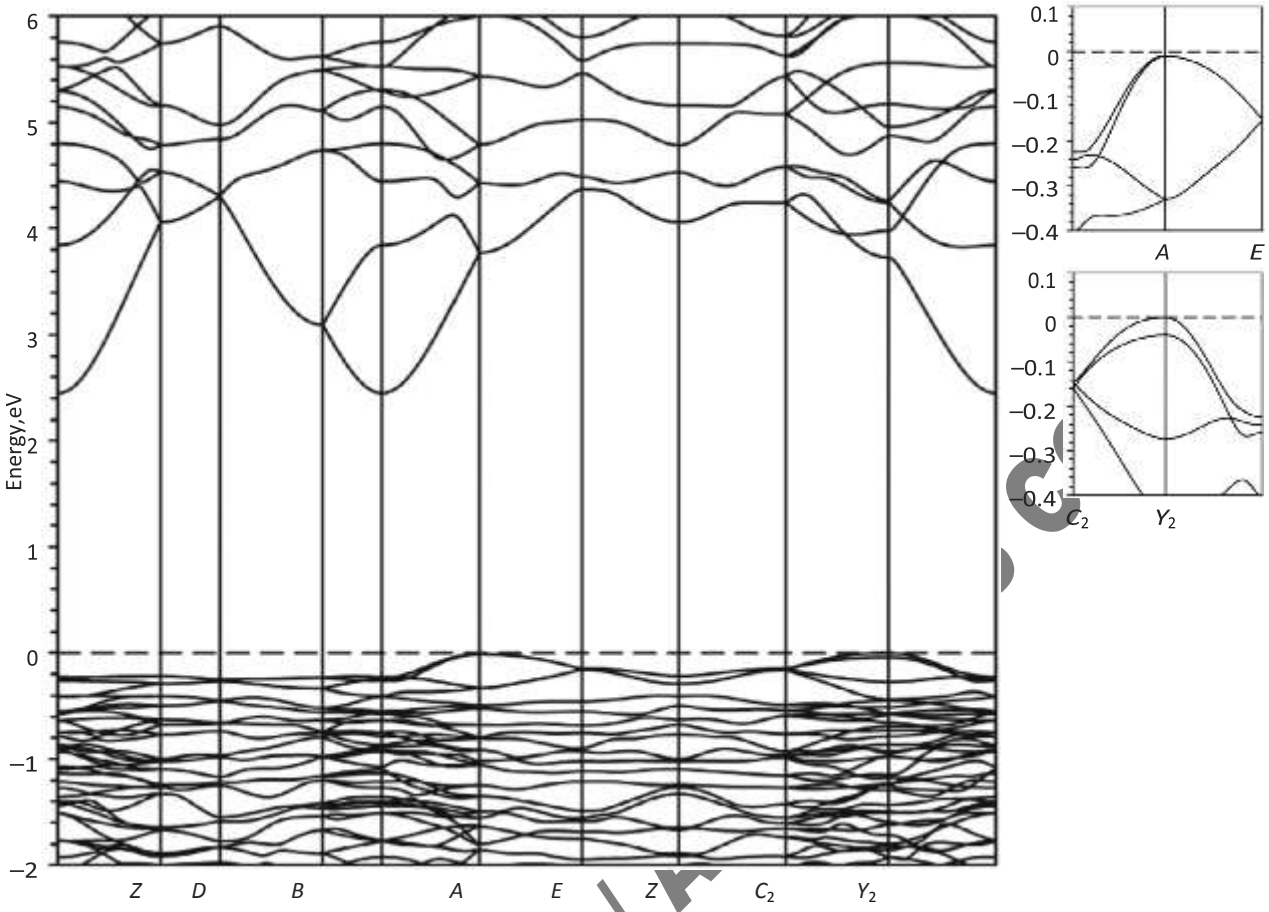

Fig. 2. Band structure of $SmGaGe_2O_7$ (the zero energy is set at the valence band top). Insets: band structure details near the valence band top.

with the same orbital quantum number for all atoms. The 4*f* states are omitted because the corresponding electrons are included in the core in the calculations and lie deep in the valence band. The density of states in the conduction band is relatively low and, for clarity of illustration, is increased by a factor of 10 in Fig. 3 to obtain a scale comparable to the valence band. The valence band is formed largely by the electronic contribution of the oxygen atoms. The contribution of the other atoms is about 12%. The region to a depth of 0.4 eV is split off the rest of the valence band and is due to charge carriers differing in effective mass. The electronic DOS at the conduction band bottom is about one order of magnitude lower than that in the region located 1 eV higher. On the whole, the electronic DOS in the conduction band is an order of magnitude lower than that in the valence band, indicating that the material has low electrical conductivity even at elevated temperatures. The low-energy contribution to the formation of the conduction band is almost the same for Ga, Ge, and O and small for Sm. With allowance for band dispersion and the traditional underestimation of the band gap in the approximations used, it is reasonable to assume that the material has low conductivity which slowly changing by temperature. This makes RE-doped digermanates attractive for optical applications.

CONCLUSIONS

Using first principles methods, we have studied for the first time the crystal structure and electronic properties of the samarium gallium digermanate $SmGaGe_2O_7$. The results demonstrate that, in the generalized gradient approximation, the structure of this compound is qualitatively and quantitatively reproduced and its space group, $P2_1/c$, persists during structural relaxation. $SmGaGe_2O_7$ is a wide-band-gap semiconductor with a 2.45 eV indirect and a 2.55 eV direct transition. Its valence band is almost completely formed by oxygen *p*-states, whereas its conduction band is formed by Ga and Ge *s*- and *p*-states with oxygen *p*-state impurities. With increasing energy, an additional contribution is made by Sm *d*-states. The

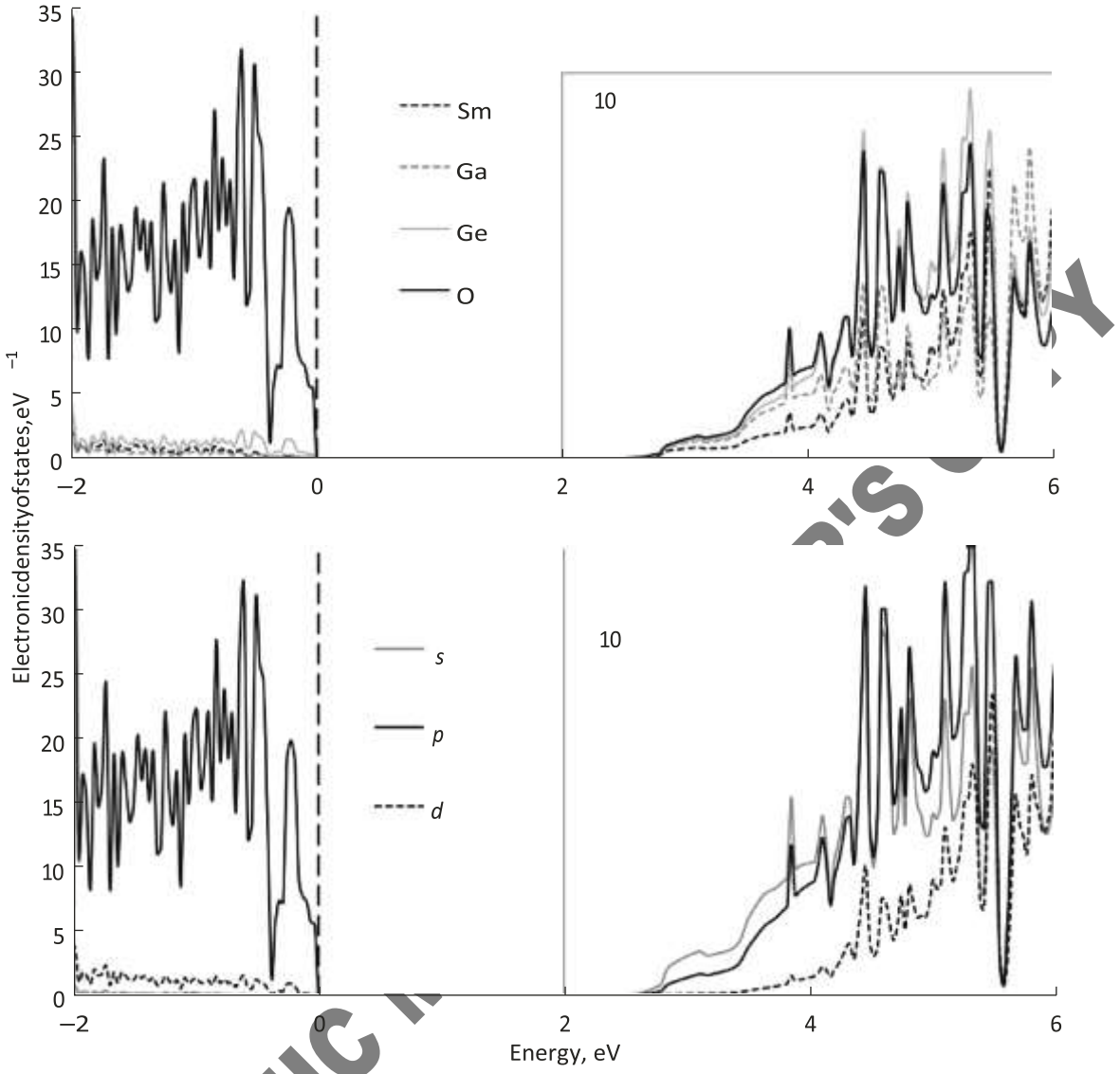

Fig. 3. Electronic density of states summed over (a) the constituent elements and (b) the contributions of orbitals (the energy zero is set at the valence band top).

structure of the valence and conduction bands leads us suggest the presence of light and heavy charge carriers. Inview of the low electronic density of states near the conduction band bottom and the traditional underestimation of the band gap in the case of exchange-correlation semilocal functionals, it is reasonable to conclude that the material has low electrical conductivity which little depends by temperature.

CONFLICT OF INTEREST

The authors declare that they have no conflicts of interest.

REFERENCES

1. Shakhno, I.V., Shevtsova, Z.N., Fedorov, P.I., andKorovin, S.S., *Khimiya i tekhnologiya redkikh i rasseyannykh elementov* (Chemistry and Technology of Rare and Trace Elements), Moscow: Vysshaya Shkola, 1976, part 2.

2. Juarez-Arellano, E.A., Bucio, L., Ruvalcaba, J.L., Moreno-Tovar, R., Garcia-Robledo, J.F., and Orozco, E., The crystal structure of $InYGe_2O_7$ germanate, *Cryst. Mater.,* 2002, vol. 217, no. 5, pp. 201–204. https://doi.org/10.1524/zkri.217.5.201.20636

3. Juarez-Arellano, E.A., Rosales, I., Bucio, L., andOrozco, E., $In_{1.08}Gd_{0.92}Ge_2O_7$: a new member of the thortveitite family, *Acta Crystallogr., Sect. C: Cryst. Struct.*

Commun., 2002, vol. C58, pp. i135–i137. https://doi.org/10.1107/S0108270102013343

4. Chang, Y.-S., Lin, H.-J., Chai, Y.-L., and Li, Y.-C.,Preparation and luminescent properties of europiumactivated $YInGe_2O_7$ phosphors, *J. Alloys Compd.,* 2008, vol. 460, nos. 1–2, pp. 421–425. https://doi.org/10.1016/j.jallcom.2007.05.060
5. Juarez-Arellano, E.A., Campa-Molina, J., Ulloa-Godinez, S., Bucio, L., and Orozco, E., Crystallochemistry of thortveitite-like and thortveitite-type compounds, *MRS Proc.,* 2005, vol. 848, pp. FF6.15.1– FF6.15.8. https://doi.org/10.1557/PROC-848-FF6.15
6. Juarez-Arellano, E.A., Rosales, I., Oliver, A., Ruvalcaba, J.L., Carbonio, R.E., Bucio, L., and Orozco, E., $In_{1.06}Ho_{0.94}Ge_2O_7$: a thortveitite-type compound, *Acta Crystallogr., Sect. C: Cryst. Struct. Commun.,* 2004, vol. C60, pp. i14–i16. https://doi.org/10.1107/S0108270103029056
7. Gaewdang, T., Chaminade, J.P., Gravereau, P., Garcia, A., Fouassier, C., Pouchard, M., Hagenmuller, P., and Jacquier, B., Structural investigations and luminescence of $In_2Ge_2O_7$ and $In_2Si_2O_7$, *J. Inorg. Gen. Chem.,* 1994, vol. 620, no. 11, pp. 1965–1970. https://doi.org/10.1002/zaac.19946201121
8. Juarez-Arellano, E.A., Bucio, L., Hernandez, J.A.,Camarillo, E., Carbonio, R.E., and Orozco, E., Synthesis, crystal structure, and preliminary study of luminescent properties of $InTbGe_2O_7$, *J. Solid State Chem.,* 2003, vol. 170, pp. 418–423. https://doi.org/10.1016/S0022-4596(02)00134-2
9. Kazei, Z.A., Kuyanov, I.A., Levitin, P.Z., Markosyan, A.S.,Mill', B.V., Reiman, S.I., Snegirev, V.V., and Tamazyan, S.A., Ordering of the iron and rare-earth magnetic subsystems and metamagnetic transitions in the $RFeGe_2O_7$ (R = Tb–Yb, Y) compounds, *Fiz. Tverd. Tela* (Leningrad), 1989, vol. 31, no. 2, pp. 105–111.
10. Cascales, C., Fernandez-Diaz, M.T., Monge, M.A.,and Bucio, L., Crystal structure and low-temperature magnetic ordering in rare earth iron germanates $RFeGe_2O_7$, R = Y, Pr, Dy, Tm, and Yb, *Chem. Mater.,* 2002, vol. 14, no. 5, pp. 1995–2003. https://doi.org/10.1021/cm0111332
11. Mill', B.V., Kazei, Z.A., Reiman, S.I., Tamazyan, S.A.,Khamdamov, F.D., and Bykova, L.Yu., Magnetic and Mössbauer studies of $RFeGe_2O_7$ (R = La–Gd) new antiferromagnetic compounds, *Vestn. Mosk. Gos. Univ., Ser. 3: Fiz. Astron.,* 1987, vol. 28, no. 4, pp. 95–98.
12. Bucio, L., Cascales, C., Alonso, J.A., and Rasines, I.,Neutron diffraction refinement and characterization of $FeRGe_2O_7$ (R = La, Pr, Nd, Gd), *J. Phys.: Condens. Matter,* 1996, vol. 8, pp. 2641–2653. https://doi.org/10.1088/0953-8984/8/15/013
13. Shih, H.R. and Chang, Y.S., Structure and photoluminescence properties of Sm^{3+} ion-doped $YInGe_2O_7$ phosphor, *Materials,* 2017, vol. 10, no. 7, p. 779. https://doi.org/10.1088/0953-8984/8/15/013
14. Yang, R.Y., Chen, H.Y., Hsiung, C.M., and Chang, S.J.,Crystalline morphology and photoluminescent properties of $YInGe_2O_7$:Eu^{3+} phosphors prepared from microwave and conventional sintering, *Ceram. Int.,* 2011, vol. 37, no. 3, pp. 749–752. https://doi.org/10.1016/j.ceramint.2010.10.001
15. Dai, P.L., Tsai, B.S., Tsai, Y.Y., Chen, H.L., Fang, T.H.,and Liao, K.H., Synthesis and luminescence properties of $YInGe_2O_7$ phosphors activated by dysprosium ions, *Opt. Mater.,* 2009, vol. 32, no. 2, pp. 392–397. https://doi.org/10.1016/j.optmat.2009.09.011
16. Lin, H.J. and Chang, Y.S., Blue-emitting phosphor of$YInGe_2O_7$ doped with Tm^{3+} ions, *Electrochem. SolidState Lett.,* 2007, vol. 10, no. 7, pp. J79–J82. https://doi.org/10.1149/1.2732076
17. Teoh, L.G., Tsai, M.T., Chang, Y.C., and Chang, Y.S.,Photoluminescence properties of Pr^{3+} ion-doped $YInGe_2O_7$ phosphor under an ultraviolet irradiation, *Ceram. Int.,* 2018, vol. 44, no. 3, pp. 2656–2660. https://doi.org/10.1016/j.ceramint.2017.10.163
18. Tsai, Y.Y., Chen, H.L., Chai, Y.L., and Chang, Y.S.,Photoluminescence properties of Bi^{3+}-doped $YInGe_2O_7$ phosphors under an ultraviolet irradiation, *Opt. Mater.,* 2013, vol. 35, no. 3, pp. 317–321. https://doi.org/10.1016/j.optmat.2012.07.010
19. Drokina, T.V., Petrakovskii, G.A., Velikanov, D.A.,and Molokeev, M.S., Specific features of magnetic ordering in the $SmFeGe_2O_7$ compound, *Phys. Solid State,* 2014, vol. 56, no. 6, pp. 1131–1136.
20. Denisova, L.T., Irtyugo, L.A., Belousova, N.V.,Beletsky, V.V., Denisov, V.M., and Kargin, Yu.F., Heat capacity and thermodynamic properties of $Yb_2Ge_2O_7$ and $Lu_2Ge_2O_7$ in the range of 350–1000 K, *Appl. Solid State Chem.,* 2018, no. 4, pp. 44–49. https://doi.org/10.18572/2619-0141-2018-4-5-44-49
21. Denisova, L.T., Irtyugo, L.A., Beletskii, V.V., Belousova, N.V., and Denisov, V.M., High-temperature heat capacity of germanates $Pr_2Ge_2O_7$ and $Nd_2Ge_2O_7$ within 350–1000 K. *Phys. Solid State,* 2018, vol. 60, no. 3, pp. 626–630. https://doi.org/10.1134/S1063783418030071
22. Denisova, L.T., Irtyugo, L.A., Kargin, Yu.F., Belousova, N.V., Beletskii, V.V., and Denisov, V.M., Synthesis and high-temperature heat capacity of $Dy_2Ge_2O_7$ and $Ho_2Ge_2O_7$, *Inorg. Mater.,* 2018, vol. 54, no. 4, pp. 361–365. https://doi.org/10.1134/S0020168518040039
23. Denisova, L.T., Kargin, Yu.F., Irtyugo, L.A., Belousova, N.V., Beletskii, V.V., and Denisov, V.M., Heat capacity of $In_2Ge_2O_7$ and $YInGe_2O_7$ from 320 to 1000 K, *Inorg. Mater.,* 2018, vol. 54, no. 12, pp. 1245–1249. https://doi.org/10.1134/S0020168518120026
24. Denisova, L.T., Irtyugo, L.A., Kargin, Yu.F.,Beletskii, V.V., and Denisov, V.M., Synthesis and high-temperature heat capacity of $Y_2Ge_2O_7$, *Russ. J. Inorg. Chem.,* 2018, vol. 63, no. 3, pp. 361–363. https://doi.org/10.1134/S003602361803004X

25. Denisova, L.T., Irtyugo, L.A., Beletskii, V.V., Belousova, N.V., and Denisov, V.M., Specific Heat of the $Er_2Ge_2O_7$–$Er_2Sn_2O_7$ Solid Solutions in the Temperature Range of 350–1000 K, *Phys. Solid State,* 2019, vol. 61, no. 4, pp. 537–540. https://doi.org/10.1134/S1063783419040061

26. Denisova, L.T., Kargin, Yu.F., Belousova, N.V., Irtyugo, L.A., Denisov, V.M., and Beletskii, V.V., Heat Capacity of the $R_2Ge_2O_7$ (R = Pr–Lu, Y) Rare-Earth Germanates, *Inorg. Mater.,* 2019, vol. 55, no. 9, pp. 952–958. https://doi.org/10.1134/S0036023619090079

27. Denisova, L.T., Irtyugo, L.A., Belousova, N.V.,Beletskii, V.V., and Denisov, V.M., High temperature heat capacity and thermodynamic properties of $Tm_2Ge_2O_7$ and $TmInGe_2O_7$ in the region of 350–1000 K, *Russ. J. Phys. Chem. A*, 2019, vol. 93, no. 3, pp. 598–601. https://doi.org/10.1134/S003602441903004X

28. Denisova, L.T., Irtyugo, L.A., Kargin, Yu.F.,Beletskii, V.V., Belousova, N.V., and Denisov V.M., Heat capacity and thermodynamic functions of $DyInGe_2O_7$ and $HoInGe_2O_7$ germanates in the temperature range 350–1000 K, *Russ. J. Inorg. Chem.,* 2019, vol. 64, no. 9, pp. 1161–1164. https://doi.org/10.1134/S0036023619090079

29. Denisova, L.T., Kargin, Yu.F., Irtyugo, L.A., Belousova, N.V., Beletskii, V.V., and Denisov, V.M., Synthesis and thermodynamic properties of germanate $Tb_2Ge_2O_7$, *Russ. J. Inorg. Chem.,* 2019, vol. 64, no. 7, pp. 886–889. https://doi.org/10.1134/S0036023619070052

30. Denisova, L.T., Molokeev, M.S., Irtyugo, L.A.,Beletskii, V.V., Belousova, N.V., and Denisov, V.M., Structure and thermodynamic properties of the $SmGaGe_2O_7$ oxide, *Phys. Solid State,* 2020, vol. 62, no. 2, pp. 384–387. https://doi.org/10.1134/S1063783420020109

31. Denisova, L.T., Molokeev, M.S., Irtyugo, L.A.,Beletskii, V.V., Kargin, Yu.F., and Denisov, V.M., Synthesis, structure, and thermophysical properties of $EuGaGe_2O_7$, *Inorg. Mater.,* 2020, vol. 56, no. 8, pp 854–858. https://doi.org/10.1134/S002016852008004X

32. Denisova, L.T., Kargin, Yu.F., Irtyugo, L.A.,Beletskii, V.V., Belousova, N.V., and Denisov, V.M., High-temperature heat capacity of the $PrFeGe_2O_7$ and $NdFeGe_2O_7$ germanates in the range 350–1000 K, *Inorg. Mater.,* 2020, vol. 56, no. 7, pp. 754–758. https://doi.org/10.1134/S0020168520070043

33. Denisova, L.T., Irtyugo, L.A., Kargin, Yu.F.,Beletskii, V.V., Belousova, N.V., and Denisov, V.M., Synthesis and high-temperature heat capacity of the $YbInGe_2O_7$ and $LuInGe_2O_7$ germanates in the range 350–1000 K, *Inorg. Mater.,* 2020, vol. 56, no. 2, pp. 151–155. https://doi.org/10.1134/S0020168520020041

34. Denisova, L.T., Irtyugo, L.A., Kargin, Yu.F.,Beletskii, V.V., Belousova, N.V., and Denisov, V.M.,

Heat Capacity and thermodynamic properties of $Gd_2Ge_2O_7$ from 350 to 1000 K, *Inorg. Mater.,* 2020, vol. 56, no. 1, pp. 62–65. https://doi.org/10.1134/S0020168520010033

35. Denisova, L.T., Irtyugo, L.A., Kargin, Yu.F.,Beletskii, V.V., Belousova, N.V., and Denisov, V.M., Synthesis and high-temperature thermodynamic properties of $InFeGe_2O_7$ and $GdFeGe_2O_7$, *Russ. J. Inorg. Chem.,* 2020, vol. 65, no. 7, pp. 955–959. https://doi.org/10.1134/S0036023620070049

36. Denisova, L.T., Kargin, Yu.F., Irtyugo, L.A.,Beletskii, V.V., Belousova, N.V., and Denisov, V.M., Germanate $NdGaGe_2O_7$: synthesis, structure, and thermophysical properties, *Russ. J. Inorg. Chem.,* 2020, vol. 65, no. 5, pp. 631–635. https://doi.org/10.1134/S0036023620050071

37. Denisova, L.T., Molokeev, M.S., Krylova, A.S., Aleksandrovskii, A.S., Irtyugo, L.A., Beletskii, V.V., and Denisov, V.M., Synthesis, crystal structure, luminescence, and thermophysical properties of $TbGaGe_2O_7$, *Phys. Solid State,* 2021, vol. 63, no. 1, pp. 75–78. https://doi.org/10.1134/S106378342101008X

38. Irtyugo, L.A., Denisova, L.T., Molokeev, M.S., Denisov, V.M., Aleksandrovskii, A.S., Beletskii, V.V., and Sivkova, E.Yu., Synthesis, crystal structure, and the optical and thermodynamic properties of $PrAlGe_2O_7$, *Russ. J. Phys. Chem. A,* 2021, vol. 95, no. 8, pp. 1546– 1550. https://doi.org/10.1134/S0036024421080124

39. Ozaki, T., Variationally optimized atomic orbitals forlarge-scale electronic structures, *Phys. Rev. B: Condens. Matter Mater. Phys.,* 2003, vol. 67, no. 15, p. 155108. https://doi.org/10.1103/PhysRevB.67.155108

40. Ozaki, T. and Kino, H., Numerical atomic basis orbitals from H to Kr, *Phys. Rev. B: Condens. Matter Mater. Phys.,* 2004, vol. 69, no. 19, p. 195113. https://doi.org/10.1103/PhysRevB.69.195113

41. Ozaki, T. and Kino, H., Efficient projector expansionfor the ab initio LCAO method, *Phys. Rev. B: Condens. Matter Mater. Phys.,* 2005, vol. 72, no. 4, p. 045121. https://doi.org/10.1103/PhysRevB.72.045121

42. Perdew, J.P., Burke, K., and Ernzerhof, M., Generalized gradient approximation made simple, *Phys. Rev. Lett.,* 1996, vol. 77, no. 18, pp. 3865–3868. https://doi.org/10.1103/PhysRevLett.77.3865